

Alma Mater Studiorum Università di Bologna  
Archivio istituzionale della ricerca

The challenging equilibrium structure of HSSH: Another success of the rotational spectroscopy / quantum chemistry synergism

This is the final peer-reviewed author's accepted manuscript (postprint) of the following publication:

*Published Version:*

Ye H., Mendolicchio M., Kruse H., Puzzarini C., Biczysko M., Barone V. (2020). The challenging equilibrium structure of HSSH: Another success of the rotational spectroscopy / quantum chemistry synergism. JOURNAL OF MOLECULAR STRUCTURE, 1211, 127933/1-127933/10 [10.1016/j.molstruc.2020.127933].

*Availability:*

This version is available at: <https://hdl.handle.net/11585/783301> since: 2020-12-04

*Published:*

DOI: <http://doi.org/10.1016/j.molstruc.2020.127933>

*Terms of use:*

Some rights reserved. The terms and conditions for the reuse of this version of the manuscript are specified in the publishing policy. For all terms of use and more information see the publisher's website.

This item was downloaded from IRIS Università di Bologna (<https://cris.unibo.it/>).  
When citing, please refer to the published version.

(Article begins on next page)

This is the final peer-reviewed accepted manuscript of:

**H. Ye, M. Mendolicchio, H. Kruse, C. Puzzarini, M. Biczysko, V. Barone. Structural properties of molecules with disulfide bond: an accurate study of HSSH. J. Mol. Struct. 1211, 127933**

The final published version is available online at:

<https://doi.org/10.1016/j.molstruc.2020.127933>

#### Terms of use:

Some rights reserved. The terms and conditions for the reuse of this version of the manuscript are specified in the publishing policy. For all terms of use and more information see the publisher's website.

*This item was downloaded from IRIS Università di Bologna (<https://cris.unibo.it/>)*

***When citing, please refer to the published version.***

# The Challenging Equilibrium Structure of HSSH: Another Success of the Rotational Spectroscopy / Quantum Chemistry Synergism

Hexu Ye<sup>1</sup>, Marco Mendolicchio<sup>2</sup>, Holger Kruse<sup>3</sup>, Cristina Puzzarini<sup>4</sup>,  
Malgorzata Biczysko<sup>1,\*</sup> and Vincenzo Barone<sup>2,\*</sup>

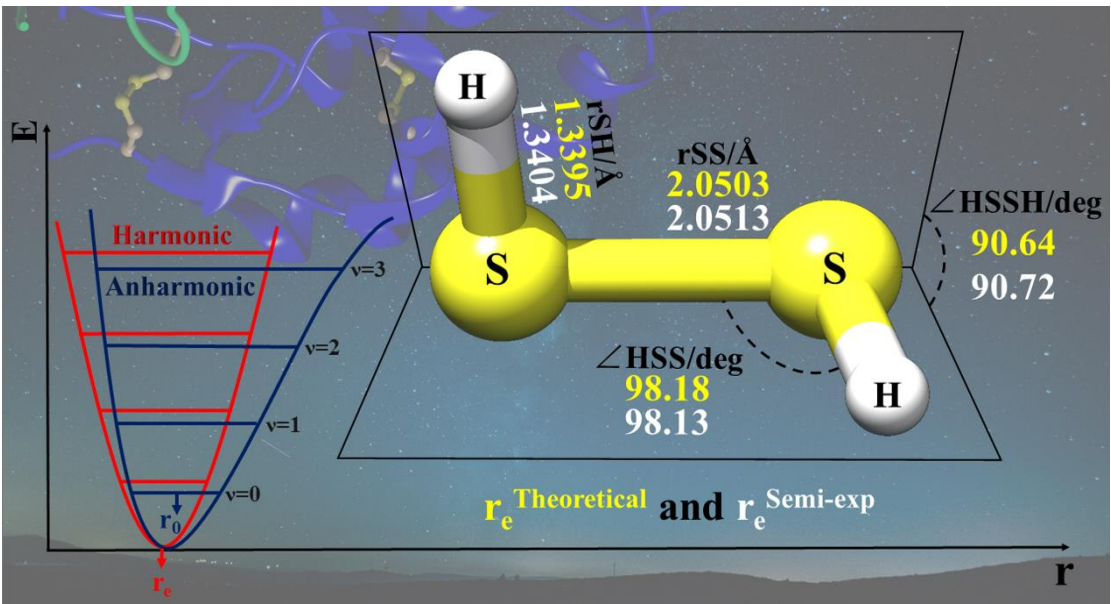
<sup>1</sup> International Centre for Quantum and Molecular Structures, Department of Physics,  
College of Sciences, Shanghai University, 99 Shangda Road, Shanghai, 200444 China

<sup>2</sup> Scuola Normale Superiore, Piazza dei Cavalieri 7, I-56126 Pisa, Italy

<sup>3</sup> Institute of Biophysics of the Czech Academy of Sciences, Královopolská 135, 612  
65 Brno, Czech Republic

<sup>4</sup> Dipartimento di Chimica “Giacomo Ciamician”, Università di Bologna,  
Via F. Selmi 2, 40126 Bologna, Italy

\*Emails: biczysko@i.shu.edu.cn, vincenzo.barone@sns.it



## Highlights

- Theoretical equilibrium structure from composite schemes
- Semi-experimental equilibrium structure
- Disulfide bond length determined with 1 mÅ accuracy

## Abstract

The simplest molecule with a disulfide bond, hydrogen disulfide (HSSH), represents an ideal test model for the determination of accurate gas-phase equilibrium structures for molecules containing third-row elements. First, pure theoretical composite schemes based on the coupled-cluster (CC) theory, which take into account the extrapolation to the complete basis set limit, core-valence correlation contributions, higher excitations in the CC expansion, and relativistic effects, allow for calculating accurate reference geometrical parameters. Second, using experimental vibrational ground-state rotational constants for a set of isotopologues, in conjunction with vibrational corrections based on second-order vibrational perturbation theory formulation and the recently developed Molecular Structure Refinement (MSR) software, we have determined the semi-experimental (SE) equilibrium structure of HSSH. The comparison of SE parameters with the computational best estimates shows an agreement within 0.001 Å for distances and 0.1 degrees for angles, thus further validating the SE approach as cost-effective, provided that the required experimental data are available. Together with the intrinsic interest of HSSH, also in connection with astrochemistry, highly accurate structural properties of a prototypical disulfide bond can serve as references for future studies of larger molecules of biological interest containing this challenging moiety.

## 1. Introduction

The covalent bond between two sulfur atoms is an important structural element in biochemistry as well as in astrochemistry. The sulfur-sulfur bond serves as a cross-link between cystine residues, thus affecting the tertiary structure of proteins. The properties of disulfide bonds in stabilizing protein conformations and formations in living cells have been reviewed by a series of works.[1-3] Furthermore, the design of disulfide-rich peptides to be used in drug design is an area of growing interest.[4] In recent years, spurred by the detection of S<sub>2</sub>H[5] in 2017, the presence of doubly sulfurated species in the interstellar medium (ISM) has been investigating. H<sub>2</sub>S<sub>2</sub> is indeed expected to be present in the ISM and cometary ices, as suggested by X-ray irradiation experiments simulating interstellar environments.[6] The detection of species including S-S bond might contribute to gain some insights on the sulfur

1 depletion problem[5, 7], and would help to improve the poor knowledge of the sulfur  
2 chemistry in the ISM. In addition, the hydrogen disulfide cation and other  
3 sulfur-containing molecules of astrochemical interest have been studied by high-level  
4 quantum-chemical calculations. [8, 9]  
5  
6

7 The accurate description of the equilibrium structure of a given molecule is a  
8 mandatory starting point for further studies on its properties and for laboratory  
9 investigations that aim at supporting its detection in astrophysical environments.  
10 Since the first experimental spectroscopic study of  $\text{H}_2\text{S}_2$  in the gas phase carried out  
11 by Wilson and Badger in 1949 [10], a series of theoretical and experimental studies  
12 aiming at revealing the structure of molecules containing the S-S covalent bond have  
13 been published[11-17], all of them agreeing in predicting a S-S bond length of  
14  $2.05 \pm 0.01 \text{ \AA}$  in  $\text{H}_2\text{S}_2$ . Although there is a large amount of data available, limited are, in  
15 number and accuracy, the determinations of the equilibrium structure, which we here  
16 recall corresponds to a minimum on the Born–Oppenheimer (BO) potential energy  
17 surface. In this article, we focus on hydrogen disulfide (HSSH), which is also known  
18 as hydrogen persulfide, dihydrogen disulfide, and disulfane, and it is the simplest  
19 molecule containing the disulfide bond. Thanks to its small size, HSSH allows for the  
20 application of high-level quantum-chemical methodologies.  
21  
22

23 On the grounds of previous experience, we will rely on methods rooted in the  
24 coupled-cluster (CC) theory including single and double excitations (CCSD) and a  
25 perturbative treatment of triple excitations (CCSD(T))[18, 19], which is often referred  
26 to as the “gold standard of quantum chemistry” for geometry optimizations.[20]  
27 CCSD(T) computations in conjunction with basis sets of triple- $\zeta$  quality can  
28 nowadays be routinely applied to medium-sized or highly-symmetric larger molecules  
29 [21, 22]. Higher accuracy can be obtained by means of the so-called composite  
30 schemes, which take into account the extrapolation to the complete basis set (CBS)  
31 limit, core-valence (CV) correlation effects and, possibly, also contributions due to  
32 higher excitations, diagonal-BO corrections or relativistic effects (see recent review  
33 for an extensive account[23]). Composite schemes can be exploited either at the  
34 energy-gradient [24, 25] or geometric-parameter level. The energy-gradient approach  
35 denoted as CCSD(T)/CBS+CV[26] is based on the Hartree-Fock self-consistent-field  
36 (HF-SCF) energy extrapolated to the CBS limit (by means of a 3-point exponential  
37 formula[27]), the CCSD(T) correlation energy extrapolated to the CBS limit (using a  
38 2-point expression[28, 29]) within the frozen-core (fc) approximation, and the  
39  
40  
41  
42  
43  
44  
45  
46  
47  
48  
49  
50  
51  
52  
53  
54  
55  
56  
57  
58  
59  
60  
61  
62  
63  
64  
65

1 inclusion of the CV correlation correction; this approach is well tested and known to  
2 be remarkably accurate.[30] An analogous scheme can be derived by applying the  
3 additivity approximation, which is at the basis of any composite approach, directly to  
4 the geometrical parameters, thus assuming that they follow that same behavior of  
5 electronic energy. The validity of these assumptions has been assessed in an extensive  
6 benchmark study.[31]

7  
8  
9  
10 The size of molecules amenable to a composite-scheme analysis can be  
11 significantly increased by incorporating the CBS and CV corrections by means of less  
12 expensive computations than CCSD(T), either within energy-gradient approaches or  
13 at the geometric-parameter level. For this purpose, the so-called “cheap” geometry  
14 scheme has been introduced [32], which accounts for the extrapolation to the CBS  
15 limit, the CV contribution and the effects of diffuse functions in the basis set using  
16 second-order Møller–Plesset perturbation theory (MP2)[33], and has been validated  
17 in several previous works, thus demonstrating good accuracy (see, e.g., Refs. [26, 34]).  
18 Similar schemes, such as the recent extension denoted as “jun-ChS” approach [35]  
19 (with reference to the jun-cc-pVnZ basis sets [36]), or analogous gradient models [37]  
20 have also been introduced. While well tested for molecules or complexes (e.g.,  
21 uracil[32], glycine[26], thiouracil[38], thiouracil-H<sub>2</sub>O[39], glycine dipeptide[40])  
22 containing at most one third-row atom, the “cheap” scheme has been applied only in  
23 one case to a system showing the noncovalent S-S bond, i.e. the DMS-SO<sub>2</sub>  
24 complex[41]. However, the covalent disulfide bond will be studied by geometry  
25 composite models for the first time in this work.

26  
27  
28  
29 From another point of view, the availability of experimental vibrational  
30 ground-state rotational constants ( $B_0$ ) for a set of isotopologues allows for exploiting  
31 the semi-experimental (SE) method, first introduced by Pulay and co-workers [42], to  
32 obtain equilibrium geometries ( $r_e^{SE}$ )[43, 44]. The SE approach is based on a nonlinear  
33 least squares fit (NLSF) of the so-called SE equilibrium rotational constants (or better  
34 of the corresponding SE equilibrium moments of inertia), which are obtained from the  
35 experimental  $B_0$ ’s corrected for the computed vibrational contributions ( $\Delta B_{vib}$ ).[45]  
36 This methodology is considered one of the best approaches to determine accurate  
37 equilibrium structures from experimental data[44, 46, 47], and can be directly  
38 compared with the equilibrium geometries issuing from quantum-chemical  
39 calculations. SE equilibrium structures have been already obtained for various  
40 sulfur-containing species [48], also including the non-covalent sulfur-sulfur

interaction [41, 47]. However, the HSSH molecule is here investigated for the first time from this point of view, thus allowing the first experimental-quality determination of a covalent S-S bond distance. The SE methodology, which avoids expensive CC computations, represents an attractive alternative to the purely theoretical approaches. It is particularly promising for the study of larger disulfide-containing molecules because of the large natural abundance of the second most abundant isotope ( $^{34}\text{S}$ ), which opens to the possibility of retrieving different sets of rotational constants in a single experimental work [49].

## 2. Methodology and Computational details

The CFOUR program package [50], Gaussian 16 suite of programs [51], PSI4 [52] as well as MRCC [53, 54] have been employed in the present study.

As mentioned in the Introduction, all composite schemes are based on CCSD(T) calculations and rely on the additivity approximation, with the various contributions being computed separately at the highest possible level. These required to employ different correlation-consistent basis sets: the valence (aug)-cc-pVnZ (n=D, T, Q, 5)[55, 56] (hereafter VnZ for cc-pVnZ and AVnZ for aug-cc-pVnZ) sets, the core-valence (aug)-cc-p(w)CVnZ (n=T, Q)[57] (abbreviated as (A)(w)CVnZ) basis sets, and the tight-d augmented cc-pV(n+d)Z (n=T, Q)[58] (V(n+d)Z in short) sets. In all composite approaches, the contributions taken into account include the extrapolation to the CBS limit [27-29], the core-valence correlation, and – in some cases – the effect of diffuse functions in the basis set.

Within the energy-gradient scheme [24] (hereafter denoted as Gradient), the additivity approximation is used to build the energy gradient to be employed in the geometry optimization:

$$\frac{dE_{\text{CBS+CV}}}{dx} = \frac{dE^{\infty}(\text{HF-SCF})}{dx} + \frac{d\Delta E^{\infty}(\text{CCSD(T)})}{dx} + \frac{d\Delta E(\text{CV})}{dx} \quad (1)$$

where  $dE^{\infty}(\text{HF-SCF})/dx$  and  $d\Delta E^{\infty}(\text{CCSD(T)})/dx$  are the energy gradients corresponding to the exponential three-point extrapolation formula by Feller[27] for the HF-SCF energy and the two-point extrapolation expression in [28, 29] for the CCSD(T) correlation contribution, respectively, with the latter evaluated within the frozen-core (fc) approximation. Core-valence correlation effects are included by adding the corresponding correction,  $d\Delta E(\text{CV})/dx$ , where the core-valence correlation energy,  $\Delta E(\text{CV})$ , is obtained as the difference between all-electron (all) and fc

CCSD(T) energies. Moreover, as an additional validation, CBS extrapolated all-electron DF-CCSD(T) (CCSD(T) method combined with the density-fitting approximation) gradients[59] in conjunction with the wCVnZ basis sets have been employed, thereby exploiting the automatic python-driven CBS gradient features of PSI4. In this model, the CCSD(T) gradient is extrapolated using the same two-point extrapolation procedure mentioned before [28, 29], while for the HF contribution the energy gradient from the largest basis set is taken. Based on the methodologies sketched above, four different gradient composite schemes have been defined, all including the CBS extrapolation of correlation energy and CV correlation contribution (either as a separate correction or inherently incorporated):

1. grad-CC-best (HF/VnZ(Q,5,6) + fc-CCSD(T)/VnZ(Q,5) + CV/CCSD(T)/CVQZ)
2. grad-CC-TQ (HF/VnZ(T,Q,5) + fc-CCSD(T)/VnZ(T,Q) + CV/CCSD(T)/CVTZ)
3. grad-dfCC-TQ (HF/wCVQZ + DF-all-CCSD(T)/wCVnZ(T,Q))
4. grad-dfCC-DT (HF/wCVTZ + DF-all-CCSD(T)/wCVnZ(D,T))

Then, the systematic trend of geometrical parameters toward the CBS limit has been exploited by making use of the assumption that their convergence has the same behavior as energy. For this purpose, analogously to the Gradient schemes, the extrapolation to the CBS limit at the HF/VnZ level is modelled by means of the three-point  $e^{-Cn}$  extrapolation formula [27], and for the CCSD(T)/(A)VnZ, CCSD(T)/CVnZ and CCSD(T)/V(n+d)Z correlation energies, the  $n^{-3}$  two-point extrapolation expression [28, 29] is used. This leads to the definition of different “geometry” schemes, where “geom-comp-CC” refers to the composite approaches equivalent to equation (1), and “geom-CC” to the models where the CBS extrapolation has been applied directly to the CCSD(T) parameters, without separating the HF-SCF and correlation contributions:

5. geom-comp-CC-best (HF/VnZ(Q,5,6) + fc-CCSD(T)/VnZ(Q,5) + CV/CCSD(T)/CVQZ)
6. geom-comp-CC-TQ (HF/VnZ(T,Q,5) + fc-CCSD(T)/VnZ(T,Q) + CV/CCSD(T)/CVTZ)
7. geom-allCC-TQ (CCSD(T)/CVnZ(T,Q))
8. geom-fcCC-Q5 (fc-CCSD(T)/VnZ(Q,5))
9. geom-fcCC-TQ (fc-CCSD(T)/VnZ(T,Q))
10. geom-fcCC-+dTQ (fc-CCSD(T)/V(n+d)Z(T,Q))

Finally, we have applied the “cheap” geometry scheme introduced in Ref. [60],



also denoted in literature as “best-cheap” or  $\text{CCSD(T)/(CBS+CV)}^{\text{MP2}}$ , and defined as:

$$r(\text{best-cheap}) = r(\text{CCSD(T)/VTZ}) + \Delta r(\text{CBS}) + \Delta r(\text{aug}) + \Delta r(\text{CV}). \quad (2)$$

This approach is based on corrections on top of the  $\text{CCSD(T)/VTZ}$  level, which are evaluated at the MP2 level and applied directly to the geometrical parameters. The considered contributions include the extrapolation to the CBS limit using the two-point extrapolation formula (with  $n=T, Q$ ):

$$\Delta r(\text{CBS}) = \frac{4^3 r(\text{MP2/VQZ}) - 3^3 r(\text{MP2/VTZ})}{4^3 - 3^3} - r(\text{MP2/VTZ}). \quad (3)$$

The effect of diffuse functions is incorporated as:

$$\Delta r(\text{aug}) = r(\text{MP2/AVTZ}) - r(\text{MP2/VTZ}), \quad (4)$$

and the core-valence correlation contribution is evaluated as follows:

$$\Delta r(\text{CV}) = r(\text{MP2/wCVTZ, all}) - r(\text{MP2/wCVTZ, valence}). \quad (5)$$

This approach is designed as:

11. geom-comp-cheap-T (fc- $\text{CCSD(T)/VTZ}$  +  $\Delta r(\text{CBS/TQ})$  +  $\Delta r(\text{aug/TZ})$  +  $\Delta r(\text{CV/wCT})$ ).

In addition to  $\text{CCSD(T)/cc-pVTZ}$ , we have also considered as starting points the  $\text{CCSD(T)/cc-pVQZ}$  and  $\text{CCSD(T)/aug-cc-pVTZ}$  levels. Moreover, the  $\Delta r(\text{CBS})$  and  $\Delta r(\text{CV})$  terms have also been computed using the augmented  $\text{AVnZ}$  ( $n=T, Q$ ) and  $\text{AwCVTZ}$  basis sets, so that the corresponding schemes do not include the additional  $\Delta r(\text{aug})$  term. Overall, these lead to the definition of two additional “cheap” models:

12. geom-comp-cheap-Q (fc- $\text{CCSD(T)/VQZ}$  +  $\Delta r(\text{CBS/Q5})$  +  $\Delta r(\text{aug/QZ})$  +  $\Delta r(\text{CV/wCT})$ )

13. geom-comp-cheap-aug (fc- $\text{CCSD(T)/AVTZ}$  +  $\Delta r(\text{CBS/AT, AQ})$  +  $\Delta r(\text{CV/AwCT})$ )

To further improve the theoretical evaluation of the equilibrium structure, the contributions due to the full (non-perturbative) treatment of triple and quadruple excitations in the CC expansion as well as relativistic effects have been considered. The first two corrections have been obtained, within the fc approximation, as the following differences in the geometrical parameters:

$$\Delta r(\text{full-T}) = r(\text{CCSDT/VTZ}) - r(\text{CCSD(T)/VTZ}) \quad (6)$$

and

$$\Delta r(\text{full-Q}) = r(\text{CCSDTQ/VDZ}) - r(\text{CCSDT/VDZ}), \quad (7)$$

where CCSDT and CCSDTQ denote the full CC singles, doubles and triples (CCSDT) [61-63], and the CC singles, doubles, triples, quadruples (CCSDTQ) [64] models, respectively. The CCSDTQ calculations required the use of the MRCC code [53, 54] interfaced to CFOUR.

The contributions due to relativistic effects have been evaluated using the lowest-order direct perturbation theory (second-order in  $1/c$ , DPT2[65]) at the MP2 level in conjunction with the uncontracted-cc-pCVQZ (hereafter denoted as uncCQZ) basis set with all electrons considered in the correlation treatment. The corresponding correction has been obtained as follows:

$$\Delta r(\text{DPT2}) = r(\text{MP2} + \text{DPT2}/\text{uncCQZ}) - r(\text{MP2}/\text{uncCQZ}). \quad (8)$$

The SE equilibrium structures have been obtained by a NLSF fit of the experimental rotational constants ( $B_0$ ) of different isotopologues corrected for the computed vibrational ( $\Delta B_{\text{vib}}$ ) and electronic ( $\Delta B_{\text{el}}$ ) contributions:

$$B_e^i = B_0^i - \Delta B_{\text{vib}}^i - \Delta B_{\text{el}}^i = B_0^i + \frac{1}{2} \sum_n \alpha_n^i - \frac{m_e}{m_p} g^i B_e^i \quad (9)$$

where  $\alpha_n^i$  denotes the vibration-rotation interaction constant [66] ( $n$  is the normal mode and  $i$  the inertial axis),  $m_e$  and  $m_p$  are the mass of the electron and proton, respectively, and  $g^i$  denotes the diagonal element of the rotational  $g$ -factor along the  $i$ -th inertial axis. The electronic corrections to the rotational constants [67] have been computed at the MP2/cc-pVTZ level. As already mentioned, the determination of SE equilibrium structures has been performed using the recently developed Molecular Structure Refinement (MSR) software [48, 68].

In order to exploit the SE approach, Density Functional Theory (DFT) and MP2 have been employed for the geometry optimization and the subsequent computation of harmonic and anharmonic force fields. To derive the vibrational contributions,  $\Delta B_{\text{vib}}^i$ 's, second-order vibrational perturbation theory (VPT2) [69, 70] has been applied to the computed anharmonic force fields. In this regard, it should be pointed out that the validity of the VPT2 treatment is not affected by the torsional motion because the corresponding barrier is of the order of 6 kcal mol<sup>-1</sup> [71], thus preventing its classification as large amplitude motion. Within the DFT approach, the standard global hybrid functional B3LYP [72] and the double-hybrid functional B2PLYP [73] with Grimme's dispersion corrections DFT-D3BJ [74], which are known to provide accurate vibrational corrections [46, 75], have been used in this work.

### 3. Results and Discussion

#### 3.1. The pure theoretical approach

The equilibrium structure parameters (their definition being provided in **Figure 1**)

obtained by means of different composite schemes are summarized in **Table 1**. The computed geometries are also compared with the experimental “ $r_e$  (partially corrected)”, structure, derived in Ref.[12] by correcting only the torsional contribution for vibrational effects, so that strictly it is not an equilibrium structure, and cannot be considered as an accurate reference for the validation of theoretical equilibrium results.

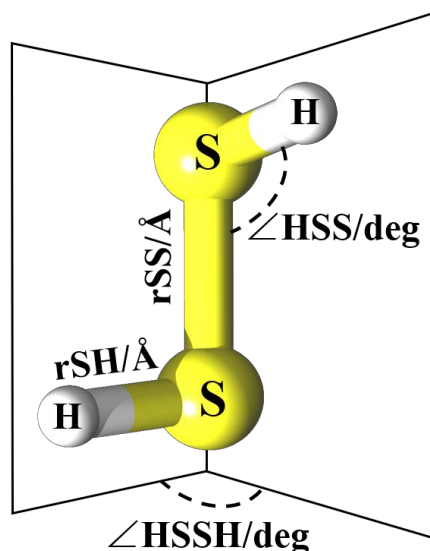


**Figure 1.** Structural parameters of hydrogen disulfide: definition of the  $r_{SS}$  and  $r_{SH}$  bond lengths, and of the  $\angle HSS$  and  $\angle HSSH$  angles.

Within the composite schemes considered, as mentioned in the computational details section, the core-valence correlation effects have been estimated with both the correlation-consistent polarized weighted wCVnZ and the standard CVnZ basis sets. By increasing  $n$ , the structural parameters calculated with these two basis sets and the corresponding CV correction converge to same values, and already with the triple- $\zeta$  basis set the difference between the two sets is quite small, as shown in Ref.[57] for the  $S_2$  molecule and in the Supporting Information (SI) for HSSH (**Table S1**). Thus, we can conclude that these two types of basis sets are equivalent for the purposes of the following discussion.

The accuracy of the Gradient composite schemes has already been verified by benchmark studies [9, 24, 76]. **Table 1** shows that the grad-CC-best and grad-CC-TQ schemes agree within 0.003 Å and 0.0003 Å for the S-S and S-H bond lengths, respectively, and within 0.05 deg for angles. This accuracy is retained also for the grad-dfCC-TQ scheme, while as expected the grad-dfCC-DT level provides results of

1 lower quality, with the S-S bond being too long by more than 0.01 Å and S-H bond  
2 too short by 0.003 Å. In general terms, the very good agreement between all  
3 gradient-based composite schemes involving all contributions obtained by basis sets  
4 of at least triple- $\zeta$  quality, further confirms their reliability in providing highly  
5 accurate reference equilibrium structures. The agreement between grad-CC-TQ and  
6 grad-dfCC-TQ shows that core-correlation effects are practically converged when  
7 using a triple- $\zeta$  basis set. In the following, we will focus our discussion on the  
8 sulfur-sulfur bond distance for which the most pronounced differences have been  
9 observed.

10 The geom-comp-CC-best and geom-comp-CC-TQ models require geometry  
11 optimizations to be carried out at the same level of theory as in the grad-CC-best and  
12 grad-CC-TQ approaches, respectively, but deal with an extrapolation to the CBS limit  
13 and core-valence effects exploited at a geometric-parameter level. It has been already  
14 noted that the bond distances from “geometry” schemes are usually shorter than those  
15 obtained from the same level gradient schemes [28], this effect being more  
16 pronounced when medium-sized basis sets (i.e.  $n=T,Q$ ) are used. This can be indeed  
17 traced back to the overestimation of the correction to basis-set truncation error in the  
18 extrapolation procedure directly applied to the structural parameters [31]. A similar  
19 trend is also observed for HSSH, the difference between these two approaches being  
20 almost negligible for the “best” ( $n=Q,5$ ) models and much larger for the schemes  
21 employing  $n=T,Q$ . In general, the S-S bond length from the grad-CC-TQ and  
22 geom-comp-CC-TQ models is shorter than its “best” counterpart, with the  
23 geom-comp-CC-TQ S-S bond length being 0.008 Å shorter than the grad-CC-TQ.  
24 Such a difference is much larger than what reported in previous studies [34, 77].  
25 While the inspection of the various contributions will be discussed later in the text, it  
26 should be noted that such a large discrepancy has to be ascribed to the extrapolated  
27 value at the HF-SCF level, the  $r(\text{HF/CBS}(T,Q,5))$  distance being 0.012 Å shorter than  
28  $r(\text{HF/CBS}(Q,5,6))$ . However, it is also important to stress that  $r(\text{HF/CBS}(T,Q,5))$  is  
29 also 0.013 Å shorter than the S-S bond length evaluated at the HF-SCF/V5Z level,  
30 which –in turn– only differs by 0.005 Å from the HF-SCF/VQZ value. Therefore, the  
31 extrapolation formula used seems to be not adequate to this specific case, and an  
32 improved result would have been obtained by assuming the HF-SCF/V5Z as CBS  
33 limit. Interestingly, and somewhat confirming the anomalous behavior addressed  
34 above, improved quality structural parameters, with the S-S bond length within 0.005  
35  
36  
37  
38  
39  
40  
41  
42  
43  
44  
45  
46  
47  
48  
49  
50  
51  
52  
53  
54  
55  
56  
57  
58  
59  
60  
61  
62  
63  
64  
65

Å from its best estimate (grad-CC-best), have been obtained for the geom-allCC-TQ geometry scheme, based on the direct extrapolation of parameters computed at the CC level, and thus inherently including core-valence correlation effects.

**Table 1.** Equilibrium structure of hydrogen disulfide, HSSH.

Method		SS (Å)	SH (Å)	HSS (deg.)	HSSH (deg.)
Gradient CBS+CV	grad-CC-best	2.0483	1.3395	98.23	90.66
	grad-CC-TQ	2.0457	1.3392	98.27	90.69
	grad-dfCC-TQ	2.0471	1.3391	98.20	90.65
	grad-dfCC-DT	2.0611	1.3365	97.89	90.63
Geometric CBS+CV	geom-comp-CC-best	2.0478	1.3395	98.25	90.63
	geom-comp-CC-TQ	2.0381	1.3386	98.27	90.72
	geom-allCC-TQ	2.0439	1.3383	98.30	90.69
Geometric CBS	geom-fcCC-Q5	2.0489	1.3406	98.32	90.62
	geom-fcCC-TQ	2.0554	1.3419	98.18	90.74
	geom-fcCC-+dTQ	2.0522	1.3417	98.26	90.71
Geometric “cheap” (CBS+CV) <sup>MP2</sup>	geom-comp-cheap-T	2.0560	1.3405	98.05	91.15
	geom-comp-cheap-Q	2.0449	1.3390	98.30	90.77
	geom-comp-cheap-aug	2.0544	1.3399	98.09	90.72
Exp <sup>a</sup> r <sub>e</sub> (partially corrected)		2.0564	1.3421	97.88	90.34

<sup>a</sup> Ref.[12].

Among the geometrical extrapolation schemes based on frozen-core computations (thus not including at all CV corrections), only the most expensive one (geom-fcCC-Q5) yields a S-S bond length within 0.001 Å with respect to the grad-CC-best approach, while the schemes based on the triple- and quadruple-ζ basis sets overestimate the S-S bond length by 0.004-0.007 Å. However, it has to be pointed out that the geom-fcCC-Q5 scheme performs very well for the wrong reason. Indeed, the difference between the CBS S-S value and the fc-CCSD(T)/V5Z distance is greater than that between the fc-CCSD(T)/V5Z and fc-CCSD(T)/VQZ bond lengths, thus suggesting an overestimation in the correction of the basis-set truncation error. Adding tight-d functions on sulfur atoms, within the geom-fcCC-+dTQ approach, allows for a faster basis set convergence than geom-fcCC-TQ, thus providing the best geom-fcCC result if one keeps in mind that the important CV contribution is missing

in such schemes. Finally, the comparison of the geom-allCC-TQ, geom-fcCC-TQ and geom-fcCC-Q5 models allows us to point out the relevance of CV effects as well as a different convergence behavior for all and fc calculations.

Moving to less expensive computational schemes, we observe that the best “cheap” approach, which in this work is labelled as geom-comp-cheap-T, shows larger deviations from grad-CC-best than those observed in previous studies, with the S-S bond too long by about 0.008 Å. We have tested possible improvements by applying CBS and CV corrections evaluated using the augmented AVnZ (n=T, Q) and AwCVTZ basis sets, and/or estimating the reference CCSD(T) term with quadruple- $\zeta$  basis set. These modifications lead to the schemes denoted as geom-comp-cheap-aug and geom-comp-cheap-Q, respectively. The geom-comp-cheap-Q method significantly improves the accuracy, but, since it involves computations at the CCSD(T)/VQZ level, it is not a viable solution for larger systems. From these attempts we can conclude that the discrepancies should be rather attributed to the initial geometry than to the CBS and CV corrections based on MP2/(A)VTZ computations.

The analysis of “geometry” composite schemes allows for better understanding the effect of the various contributions on the overall molecular structure. For the geom-comp-CC-best and geom-comp-CC-TQ approaches, these are reported in **Table 2**. The role of different contributions in the geom-comp-cheap-T method (reported in **Table 3**) is better highlighted by re-writing equation (2) as:

$$r(\text{geom-comp-cheap-T}) = \Delta r(\text{CBS}) + \Delta r(\text{T}) + \Delta r(\text{aug}) + \Delta r(\text{CV}) \quad (9)$$

where

$$\Delta r(\text{T}) = r(\text{CCSD(T)/cc-pVTZ}) - r(\text{MP2/cc-pVTZ})$$

From **Table 2**, it is apparent that the S-S bond length is the most sensitive parameter to the change of the basis-set size, especially for the HF-SCF extrapolation to the CBS limit, as already addressed above. For all bond lengths and angles, the CCSD(T) electron correlation contribution is smaller when extrapolations are carried out with larger basis sets; however, the differences lie nearly within 0.001 Å for distances (0.0002 Å for S-H) and within 0.1 deg. for angles. Concerning the CV correlation contribution, which has been evaluated by employing the CVnZ basis sets, the convergence seems to be not yet completely achieved at the CCSD(T)/CVQZ level for S-S. Indeed, the CV correction computed with the CVQZ basis set decreases the S-S bond length by 0.0049 Å, thus by 0.001 Å more than its CVTZ counterpart.

On the other hand, such a correction differs by only 0.0003 Å for the S-H distance.

**Table 2.** Different contributions in the geom-comp-CC-best and geom-comp-CC-TQ schemes.

geom-comp-CC-best	HF/CBS(Q,5,6)	$\Delta f_c$ -CCSD(T)/CBS(Q,5)	CV(CCSD(T)/CVQZ)
SS (Å)	2.0495	+0.0032	-0.0049
SH (Å)	1.3271	+0.0146	-0.0021
HSS (deg.)	99.07	-0.83	+0.01
HSSH (deg.)	89.96	+0.66	+0.01
geom-comp-CC-TQ	HF/CBS(T,Q,5)	$\Delta f_c$ -CCSD(T)/CBS(T,Q)	CV(CCSD(T)/CVTZ)
SS (Å)	2.0373	+0.0046	-0.0038
SH (Å)	1.3255	+0.0148	-0.0017
HSS (deg.)	99.16	-0.89	+0.00
HSSH (deg.)	89.96	+0.75	+0.01

From **Table 3** one can notice that, at the MP2 level, the corrections due to the extrapolation to the CBS limit above the MP2/VQZ level shorten the S-S and S-H bond lengths by 0.010 Å and 0.001 Å, respectively, whereas the HSS and HSSH angles increase by 0.17 and 0.11 degrees, respectively. The effect due to triples,  $\Delta r(T)$ , provides the largest correction in this model, with contributions of +0.0174 Å for the S-S bond and +0.005 Å for the S-H distance. As expected, core-valence correlation decreases bond lengths. The CV contributions from MP2 calculations in conjunction with a triple- $\xi$  basis set are similar to the CV(CCSD(T)/CVQZ) results, reported in **Table 2**. The effects of diffuse functions at the MP2 level are very small; therefore, the inclusion of corresponding correction in the geom-comp-cheap-aug scheme does not lead to any improvement with respect to geom-comp-cheap-T.

**Table 3.** Different contributions in the geom-comp-cheap-T method.

	MP2/VTZ	MP2/VQZ	MP2/CBS	$\Delta r(T)$	$\Delta r(aug)$	$\Delta r(CV)$
SS (Å)	2.0654	2.0525	2.0430	+0.0171	+0.0013	-0.0054
SH (Å)	1.3394	1.3379	1.3368	+0.0050	+0.0008	-0.0021
HSS (deg.)	97.80	98.03	98.20	-0.09	-0.04	-0.02
HSSH (deg.)	90.64	90.78	90.89	-0.09	+0.30	+0.05

**Table 4.** Effect of diffuse functions on the geometry of HSSH, calculated at the CCSD(T) level.

n	VnZ	rSS (Å)		VnZ	rSH (Å)	
		AVnZ	$\Delta r^a$		AVnZ	$\Delta r^a$
D	2.1102	2.1211	0.0109	1.3571	1.3592	0.0022
T	2.0825	2.0840	0.0015	1.3444	1.3454	0.0010
Q	2.0668	2.0674	0.0006	1.3430	1.3434	0.0005
5	2.0581	2.059 <sup>d</sup>	0.0009	1.3418	1.342 <sup>d</sup>	0.0002
n	VnZ	$\angle$ HSS (deg.)		VnZ	$\angle$ HSSH (deg.)	
		AVnZ	$\Delta\theta^b$		AVnZ	$\Delta\phi^c$
D	97.45	97.14	0.32	90.50	91.12	0.62
T	97.71	97.66	0.05	90.55	90.80	0.25
Q	97.98	97.98	0.00	90.66	90.70	0.04
5	98.15	98.1 <sup>d</sup>	0.05	90.64	90.7 <sup>d</sup>	0.06

<sup>a</sup>  $\Delta r = r[\text{AVnZ}] - r[\text{VnZ}]$ ; <sup>b</sup>  $\Delta\theta = \theta[\text{AVnZ}] - \theta[\text{VnZ}]$ ; <sup>c</sup>  $\Delta\phi = \phi[\text{AVnZ}] - \phi[\text{VnZ}]$ ; <sup>d</sup> Ref. [76].

It is also worth investigating the role of diffuse functions at the CCSD(T) level. As can be seen in **Table 4**, their effect is large when basis sets of double- $\zeta$  quality are used, but it decreases rapidly as the size of the basis set increases, their contribution being very small with quadruple- $\zeta$  or larger basis sets. As a consequence, the HSSH structural parameters derived from standard VnZ and augmented AVnZ basis sets converge toward the same value, and their difference monotonically decreases toward zero. Note that the CCSD(T)/AV5Z results have been reported in Ref.[71] with a too optimistic precision of 0.001 Å and 0.1 deg. The comparison of the results of **Table 4** with those collected in **Table 3** allows us to conclude that, as expected, MP2 parameters converge faster than their CCSD(T) counterparts when increasing the dimension of the basis set. This trend suggests that  $\Delta r(\text{T})$  in **Table 3** is overestimated and could explain why the “cheap” scheme behaves unsatisfactorily for the S-S bond.

From the discussion above, it is clear that the S-S distance is the most difficult parameter to describe accurately, with the values from different methodologies ranging between 2.0381 and 2.0611Å. By comparing all the results, it is apparent that the grad-CC-best approach is the most expensive and the most accurate one; however, it has to be noted that the geom-comp-CC-best approach involves the various



contributions at the same level and shows similar results. Despite the fact that the grad-CC-TQ and grad-dfCC-TQ schemes do not require CCSD(T)/V5Z computations, yet they provide results in close agreement with grad-CC-best. Since the grad-CC-best scheme is the best computational approach used in this work, in order to obtain our final pure theoretical estimate, we have applied to it the corrections due to the full treatment of triples and quadruples in the CC expansion and to the relativistic effects, as explained in the computational details section. The results are summarized in **Table 5**. From the inspection of this table, it is evident that, while the full-T corrections are very small for all distances (i.e. less than 0.001 Å), the full-Q and DPT2 contributions are not negligible for the S-S bond (+0.0025 altogether). The overall correction is null for the S-H distance and amounts to +0.002 Å for S-S. For the HSS angle, the three contributions lead to a decrease of 0.05 deg., while the decreasing reduces to 0.02 deg. for the HSSH dihedral angle.

**Table 5.** Full-T, full-Q, and DPT2 corrections applied to the grad-CC-best scheme.

	grad-CC-best	full-T	full-Q	DPT2	best estimate
SS (Å)	2.0483	-0.0005	+0.0015	+0.0010	2.0503
SH (Å)	1.3395	-0.0006	+0.0006	+0.0000	1.3395
HSS (deg.)	98.23	+0.05	-0.03	-0.07	98.18
HSSH (deg.)	90.66	-0.03	+0.03	-0.02	90.64

In the following the “best estimate” of **Table 5** is taken as a reference for the semi-experimental study, which will be performed employing different methods in conjunction with the (A)VTZ basis sets in the derivation of the vibrational corrections, with the final aim of obtaining the best compromise between accuracy and computational cost.

### 3.2. The semi-experimental approach

*Winnewisser et al.* [12] reported the experimental rotational constants ( $B_0^{\text{exp}}$ ) for HSSH and for three isotopic species (the mono-substituted  $^{34}\text{S}$  and D isotopologues, and the doubly-substituted D isotopic species), thus making it possible to determine the full SE equilibrium structure. As mentioned in the computational details section, all experimental rotational constants have been corrected for vibrational and

1 electronic contributions in order to derive the corresponding SE equilibrium rotational  
2 constants. For evaluating the  $\Delta B_{\text{vib}}$  corrections, anharmonic force fields have been  
3 computed at the B3LYP(-D3BJ), B2LYP(-D3BJ) and MP2 levels in conjunction with  
4 (A)VTZ basis sets, while as already mentioned the  $\Delta B_{\text{el}}$  corrections have been  
5 calculated at the MP2/VTZ level. All  $\Delta B_{\text{vib}}$  and  $\Delta B_{\text{el}}$  contributions together with all  
6  $B_0^{\text{exp}}$ 's are collected in the SI (**Table S2**). In the fitting procedure, when an  
7 isotopologue presents vibrational contributions very different from the other isotopic  
8 species, its moments of inertia may be poorly fitted, therefore the reweighting scheme  
9 has been chosen in order to adjust the weights of the SE moments of inertia. The SE  
10 equilibrium structures of HSSH, obtained using different levels of theory for the  
11 vibrational corrections, are summarized in **Table 6**. It is, first of all, noted that the  
12 vibrational corrections calculated by means of different levels of theory lead to very  
13 similar structural parameters, bond lengths agreeing within 0.001 Å and valence  
14 angles within 0.2 deg. Vibrational corrections calculated at the MP2/VTZ level lead to  
15 the shortest S-S bond length (2.0512 Å) and the smallest HSSH dihedral angle (90.65  
16 deg). The standard deviation, 95% confidence interval and condition number,  
17 obtained from the error analysis performed by MSR and reported in **Table 6**, confirm  
18 the reliability of the determined structural parameters.

19 The mean absolute error (MAE) and maximum absolute deviations ( $|\text{MAX}|$ ), with  
20 respect to the “best estimate” structure, for the  $r_e^{\text{SE}}$  bond lengths and angles as well as  
21 for the corresponding pure theoretical parameters computed at the levels of theory  
22 (DFT and MP2) used for the evaluation of the vibrational corrections are shown in  
23 **Table S3** (in the SI) and **Figure 2**. Concerning the later, we note that the SE approach  
24 always leads to a good agreement with the reference structure independently of the  
25 intrinsic accuracy of the geometries optimized at the level of theory used for  
26 computing vibrational corrections. Moreover, SE structural parameters are closer to  
27 the reference (“best estimate”) than those optimized at the CCSD(T)/AV5Z level (see  
28 **Table 4**). In other words, for HSSH, the SE approach allows for obtaining results  
29 better than those issuing from B2PLYP, B3LYP, MP2 and even CCSD(T) geometry  
30 optimizations. Moreover, it is further confirmed that vibrational corrections calculated  
31 by different methods lead to equivalent SE results.

**Table 6.** SE equilibrium structure of HSSH.

VTZ					
	B2PLYP	B2PLYP-D3BJ	B3LYP	B3LYP-D3BJ	MP2
SS (Å)	2.0513 (4;9) <sup>a</sup>	2.0513 (3;7)	2.0515 (9;20)	2.0516 (7;14)	2.0512 (1;3)
SH (Å)	1.3404 (22;48)	1.3403 (18;40)	1.3401 (47;105)	1.3399 (35;77)	1.3408 (8;17)
HSS (deg.)	98.13 (2;4)	98.12 (2;4)	98.07 (4;10)	98.04 (3;7)	98.19 (1;1)
HSSH (deg.)	90.72 (2;5)	90.72 (2;5)	90.74 (5;12)	90.75 (4;9)	90.65 (1;2)
Condition number	10	11	11	10	10

AVTZ					
	B2PLYP	B2PLYP-D3BJ	B3LYP	B3LYP-D3BJ	MP2
SS(Å)	2.0514 (3;7)	2.0513 (3;7)	2.0517 (6;13)	2.0516 (7;17)	2.0514 (6;13)
SH(Å)	1.3401 (14;32)	1.3403 (14;31)	1.3398 (33;73)	1.3400 (42;94)	1.3404 (26;56)
HSS (deg)	98.07 (2;3)	98.13 (2;4)	98.02 (3;6)	98.06 (4;8)	98.09 (3;6)
HSSH (deg)	90.72 (2;5)	90.72 (2;5)	90.72 (4;9)	90.75 (5;10)	90.72 (4;9)
Condition number	10	10	10	11	10

<sup>a</sup> In parentheses both the standard deviation (first value) and the confidence interval at a 95% confidence level (second value), rounded to  $1 \times 10^{-5}$  Å for bond lengths and  $1 \times 10^{-3}$  degrees for angles if smaller than these values.

## 4. Conclusions

By comparing the equilibrium structural parameters of HSSH as obtained by

means of a series of composite schemes, it can be concluded that an accurate description of the covalent sulfur-sulfur bond is quite challenging, with non-negligible contributions obtained from the very expensive CCSDTQ method and from the relativistic effects. The most accurate results, derived from the grad-CC-best scheme with the inclusion of the full-T, full-Q and DPT2 corrections, are: S-S=2.0503 Å, S-H=1.3395 Å, HSS=98.18 deg., and HSSH=90.64 deg. Compared with the grad-CC-best model, the “cheap” geometry schemes starting from CCSD(T)/(A)VTZ equilibrium structures and including CBS and CV corrections based on MP2 computations show results of lower quality than those to which we are accustomed for molecules containing at most one third-row atom. This further confirms that molecules with a S-S bond are still a challenge for quantum-chemical computations. At variance, the SE approach yields always consistent results, irrespective of the level of theory used to compute vibrational corrections, also leading to structural parameters more accurate than CCSD(T)/AV5Z geometry optimizations, especially for what concerns the S-S distance.

In conclusion, thanks to a very effective combination of reliability and low computational cost, the SE approach can be recommended as a viable route for the determination of accurate molecular structures for a larger panel of species involving sulfur-sulfur bonds, which will be considered in our follow-up studies.

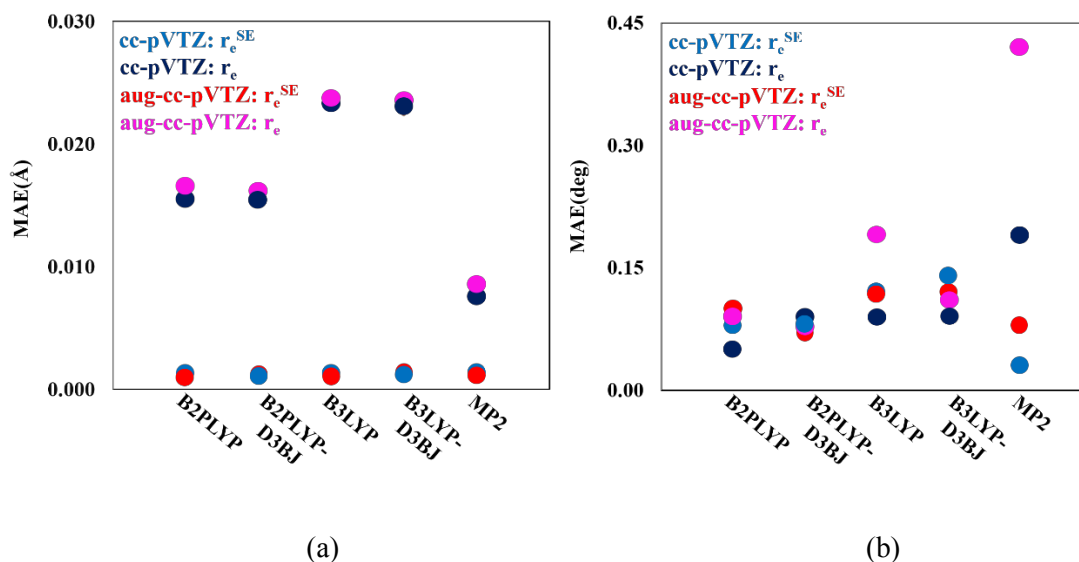


**Figure 2.** (a) Mean absolute error (MAE) for bond lengths (Å) and (b) for angles (deg.) with respect to “best estimate” parameters for SE equilibrium (light blue and red) and computed equilibrium (dark blue and pink) parameters at the B2PLYP-D3BJ/(A)VTZ, B3LYP-D3BJ/(A)VTZ, and MP2/(A)VTZ levels.

## Acknowledgments

This work is dedicated to the memory of Dr. Jon T. Hougen, a great scientist and an inspiring person. This work was enabled by the financial support from the National Natural Science Foundation of China (Grant No. 31870738). In Pisa and Bologna, this work has been supported by MIUR “PRIN 2015” funds (Grant Number 2015F59J3R). HK acknowledges support by the ERDF project SYMBIT (CZ.02.1.01/0.0/0.0/15\_003/0000477).

## References:

- [1] T. E. Creighton, Disulphide bonds and protein stability, *BioEssays* 8(2-3) (1988) 57-63.
- [2] C. S. Sevier, C. A. Kaiser, Formation and transfer of disulphide bonds in living cells, *Nat. Rev. Mol. Cell Biol.* 3(11) (2002) 836.
- [3] D. Witt, Recent developments in disulfide bond formation, *Synthesis* 2008(16) (2008) 2491-2509.
- [4] S. E. Northfield, C. K. Wang, C. I. Schroeder, T. Durek, Meng-Wei. Kan, J. E. Swedberg, D. J. Craik, Disulfide-rich macrocyclic peptides as templates in drug design, *Eur. J. Med. Chem.* 77 (2014) 248-257.
- [5] A. Fuente, J. R. Goicoechea, J. Pety, R. Le Gal, R. Martin-Domenech, P. Gratier, V. Guzman, E. Roueff, J. C. Loison, G. M. M. Caro, V. Wakelam, M. Gerin, P. Riviere-Marichalar, T. Vidal, First Detection of Interstellar S<sub>2</sub>H, *Astrophys. J., Lett.* 851(2) (2017) L49.
- [6] A. Jimenez-Escobar, G. M. M. Caro, A. Ciaravella, C. Cecchi-Pestellini, R. Candia, G. Micela, Soft X-Ray Irradiation of H<sub>2</sub>S Ice and the Presence of S<sub>2</sub> in Comets, *Astrophys. J., Lett.* 751(2) (2012) L40.
- [7] R. Martín-Doménech, I. Jiménez-Serra, G. M. M. Caro, H. S. P. Müller, A. Occhiogrosso, L. Testi, P. M. Woods, S. Viti, The sulfur depletion problem: upper limits on the H<sub>2</sub>S<sub>2</sub>, HS<sub>2</sub><sup>-</sup>, and S<sub>2</sub> gas-phase abundances toward the low-mass warm core IRAS 16293-2422, *Astron. Astrophys.* 585 (2016) A112.
- [8] R. C. Fortenberry, J. S. Francisco, A Possible Progenitor of the Interstellar Sulfide Bond: Rovibrational Characterization of the Hydrogen Disulfide Cation HSSH<sup>+</sup>, *Astrophys. J.* 856(1) (2018) 30.
- [9] S. Alessandrini, J. Gauss, C. Puzzarini, Accuracy of Rotational Parameters Predicted by High-Level Quantum-Chemical Calculations: Case Study of Sulfur-Containing Molecules of Astrochemical Interest, *J. Chem. Theory Comput.* 14(10) (2018) 5360-5371.
- [10] M. K. Wilson, R. M. Badger, The Infra-Red Spectrum and Molecular Configuration of Hydrogen Persulfide, *J. Chem. Phys.* 17(12) (1949) 1232-1236.
- [11] A. Hinchliffe, Structure and properties of HSSH, H<sub>2</sub>SS, FSSF and F<sub>2</sub>SS, *J. Mol. Struct.* 55 (1979) 127-134.
- [12] G. Winnewisser, K. M. T. Yamada, Millimetre, submillimetre and infrared spectra of disulphane (HSSH) and its isotopic species, *Vib. Spectrosc.* 1(3) (1991) 263-272.

- [13] P. Birner, H. J. Köhler, A. Karpfen, H. Lischka, An ab initio study of the polysulfane series  $H_2S_2$  to  $H_2S_6$  and of  $S_8$ , *J. Mol. Struct.: THEOCHEM* 226(3-4) (1991) 223-239.
- [14] G. I. Cárdenas-Jirón, C. Cárdenas-Lailhacar, A. Toro-Labbé, Theoretical analysis of the internal rotation, molecular structures and electronic properties of the XSSX series of molecules (X= H, F, Cl), *J. Mol. Struct.: THEOCHEM* 282(1-2) (1993) 113-122.
- [15] J. Koput, An ab initio study on the equilibrium structure and torsional potential energy function of disulfane, *Chem. Phys. Lett.* 259(1-2) (1996) 146-150.
- [16] J. Zhang, X. Li, Q. Gou, G. Feng, Disulfide Bond in Diethyl Disulfide: A Rotational Spectroscopic Study, *J. Phys. Chem. A* 122(25) (2018) 5597-5601.
- [17] J. Demaison, N. Vogt, R. T. Saragi, M. Juanes, H. D. Rudolph, A. Lesarri, The S– S Bridge: A Mixed Experimental - Computational Estimation of the Equilibrium Structure of Diphenyl Disulfide, *Chemphyschem* 20(3) (2019) 366-373.
- [18] G. D. Purvis III, R. J. Bartlett, A full coupled-cluster singles and doubles model: the inclusion of disconnected triples, *J. Chem. Phys. Lett.* 76(4) (1982) 1910-1918.
- [19] K. Raghavachari, G. W. Trucks, J. A. Pople, M. Head-Gordon, A fifth-order perturbation comparison of electron correlation theories, *Chem. Phys. Lett.* 157(6) (1989) 479-483.
- [20] K. A. Peterson, D. Feller, D. A. Dixon, Chemical accuracy in ab initio thermochemistry and spectroscopy: current strategies and future challenges, *Theor. Chem. Acc.* 131(1) (2012).
- [21] H. Kruse, J. Sponer, Highly accurate equilibrium structure of the  $C_{2h}$  symmetric N1-to-O2 hydrogen-bonded uracil-dimer, *Int. J. Quantum. Chem.* 118(15) (2018).
- [22] P. R. Spackman, D. Jayatilaka, A. Karton, Basis set convergence of CCSD(T) equilibrium geometries using a large and diverse set of molecular structures, *J. Chem. Phys.* 145(10) (2016).
- [23] A. J. C. Varandas, Straightening the Hierarchical Staircase for Basis Set Extrapolations: A Low-Cost Approach to High-Accuracy Computational Chemistry, *Annu Rev Phys Chem* 69 (2018) 177-203.
- [24] M. Heckert, M. Kállay, D. P. Tew, W. Klopper, J. Gauss, Basis-set extrapolation techniques for the accurate calculation of molecular equilibrium geometries using coupled-cluster theory, *J. Chem. Phys.* 125(4) (2006) 044108.
- [25] M. Heckert, M. Kállay, J. Gauss, Molecular equilibrium geometries based on coupled-cluster calculations including quadruple excitations, *Mol. Phys.* 103(15-16) (2005) 2109-2115.
- [26] V. Barone, M. Biczysko, J. Bloino, C. Puzzarini, The performance of composite schemes and hybrid CC/DFT model in predicting structure, thermodynamic and spectroscopic parameters: the challenge of the conformational equilibrium in glycine, *Phys. Chem. Chem. Phys.* 15(25) (2013) 10094.
- [27] D. Feller, The use of systematic sequences of wave functions for estimating the complete basis set, full configuration interaction limit in water, *J. Chem. Phys.* 98(9) (1993) 7059-7071.
- [28] T. Helgaker, W. Klopper, H. Koch, J. Noga, Basis-set convergence of correlated calculations on water, *J. Chem. Phys.* (23) (1997) 9639-9646.
- [29] A. Halkier, T. Helgaker, P. Jørgensen, W. Klopper, H. Koch, J. Olsen, A. K. Wilson, Basis-set convergence in correlated calculations on Ne,  $N_2$ , and  $H_2O$ , *Chem. Phys. Lett.* 286(3-4) (1998) 243-252.
- [30] C. Puzzarini, J. F. Stanton, J. Gauss, Quantum-chemical calculation of spectroscopic parameters for rotational spectroscopy, *Int. Rev. Phys. Chem.* 29(2) (2010) 273-367.
- [31] C. Puzzarini, Extrapolation to the Complete Basis Set Limit of Structural Parameters: Comparison

- of Different Approaches, *J. Phys. Chem. A* 113(52) (2009) 14530-14535.
- [32] C. Puzzarini, V. Barone, Extending the molecular size in accurate quantum-chemical calculations: the equilibrium structure and spectroscopic properties of uracil, *Phys. Chem. Chem. Phys.* 13(15) (2011) 7189-7197.
- [33] C. Møller, M. S. Plesset, Note on an Approximation Treatment for Many-Electron Systems, *Phys. Rev.* 46 (1934) 618-622.
- [34] V. Barone, M. Biczysko, J. Bloino, C. Puzzarini, Accurate molecular structures and infrared spectra of trans-2,3-dideuterooxirane, methyloxirane, and trans-2,3-dimethyloxirane, *J. Chem. Phys.* 141(3) (2014).
- [35] S. Alessandrini, V. Barone, C. Puzzarini, Extension of the “cheap” composite approach to non-covalent interactions: the jun-ChS scheme, *J. Chem. Theory Comput.* (2019).
- [36] E. Papajak, H. R. Leverentz, J. J. Zheng, D. G. Truhlar, Efficient Diffuse Basis Sets: cc-pVxZ plus and maug-cc-pVxZ, *J. Chem. Theory Comput.* 5(5) (2009) 1197-1202.
- [37] P. Kraus, I. Frank, Validating additive correction schemes against gradient-based extrapolations, *Int. J. Quantum. Chem.* 119(16) (2019).
- [38] C. Puzzarini, M. Biczysko, V. Barone, I. Peña, C. Cabezas, J. L. Alonso, Accurate molecular structure and spectroscopic properties of nucleobases: a combined computational–microwave investigation of 2-thiouracil as a case study, *Phys. Chem. Chem. Phys.* 15(39) (2013) 16965-16975.
- [39] C. Puzzarini, M. Biczysko, Microsolvation of 2-Thiouracil: Molecular Structure and Spectroscopic Parameters of the Thiouracil-Water Complex, *J. Phys. Chem. A* 119(21) (2015) 5386-5395.
- [40] C. Puzzarini, M. Biczysko, V. Barone, L. Largo, I. Peña, C. Cabezas, J. Alonso, Accurate characterization of the peptide linkage in the gas phase: A joint quantum-chemical and rotational spectroscopy study of the glycine dipeptide analogue, *J. Phys. Chem. Lett.* 5(3) (2014) 534-540.
- [41] D. A. Obenchain, L. Spada, S. Alessandrini, S. Rampino, S. Herbers, N. Tasinato, M. Mendolicchio, P. Kraus, J. Gauss, C. Puzzarini, J. U. Grabow, V. Barone, Unveiling the Sulfur-Sulfur Bridge: Accurate Structural and Energetic Characterization of a Homochalcogen Intermolecular Bond, *Angew. Chem. Int. Edit* 57(48) (2018) 15822-15826.
- [42] P. Pulay, W. Meyer, J. E. Boggs, Cubic force constants and equilibrium geometry of methane from Hartree–Fock and correlated wavefunctions, *J. Chem. Phys.* 68(11) (1978) 5077-5085.
- [43] J. Demaison, J. E. Boggs, A. G. Csaszar, Equilibrium molecular structures: from spectroscopy to quantum chemistry, CRC Press(2016).
- [44] F. Pawłowski, P. Jørgensen, J. Olsen, F. Hegelund, T. Helgaker, J. Gauss, K. L. Bak, J. F. Stanton, Molecular equilibrium structures from experimental rotational constants and calculated vibration–rotation interaction constants, *J. Chem. Phys.* 116(15) (2002) 6482-6496.
- [45] J. Demaison, Experimental, semi-experimental and ab initio equilibrium structures, *Mol. Phys.* 105(23-24) (2007) 3109-3138.
- [46] M. Piccardo, E. Penocchio, C. Puzzarini, M. Biczysko, V. Barone, Semi-Experimental Equilibrium Structure Determinations by Employing B3LYP/SNSD Anharmonic Force Fields: Validation and Application to Semirigid Organic Molecules, *J. Phys. Chem. A* 119(10) (2015) 2058-2082.
- [47] P. Kraus, D. A. Obenchain, I. Frank, Benchmark-Quality Semiexperimental Structural Parameters of van der Waals Complexes, *J. Phys. Chem. A* 122(4) (2018) 1077-1087.
- [48] E. Penocchio, M. Mendolicchio, N. Tasinato, V. Barone, Structural features of the carbon-sulfur chemical bond: a semi-experimental perspective, *Can. J. Chem.* 94(12) (2016) 1065-1076.

- [49] J. Zhang, H. Ye, Y. Jin, Q. Gou, M. Biczysko, G. Feng, Conformational Equilibria and Molecular Structures of Model Sulfur-Sulfur Bridge Systems: Diisopropyl Disulfide, *J. Phys. Chem. A* 123(50) (2019) 10714-10720.
- [50] CFOUR, a quantum-chemical program package by J. F. Stanton, J. Gauss, M. E. Harding, M. E. P. G. Szalay with contributions from A. A. Auer, R. J. Bartlett, U. Benedikt, C. Berger, D. E. Bernholdt, Y. J. Bomble, L. Cheng, O. Christiansen, M. Heckert, O. Heun, C. Huber, T. -C. Jagau, D. Jonsson, J. Jusélius, K. Klein, W. J. Lauderdale, D. A. Matthews, T. Metzroth, L. A. Mück, D. P. O'Neill, D. R. Price, E. Prochnow, C. Puzzarini, K. Ruud, F. Schiffmann, W. Schwalbach, S. Stopkiewicz, A. Tajti, J. Vázquez, F. Wang, J. D. Watts and the integral packages MOLECULE (J. Almlöf and P. R. Taylor), PROPS (P. R. Taylor), ABACUS (T. Helgaker, H. J. Aa. Jensen, P. Jørgensen, and J. Olsen), and ECP routines by A. V. Mitin and C. van Wüllen. For the current version, see <http://www.cfour.de>.
- [51] M. J. Frisch, G. W. Trucks, H. B. Schlegel, G. E. Scuseria, M. A. Robb, J. R. Cheeseman, G. Scalmani, V. Barone, G. A. Petersson, H. Nakatsuji, X. Li, M. Caricato, A. V. Marenich, J. Bloino, B. G. Janesko, R. Gomperts, B. Mennucci, H. P. Hratchian, J. V. Ortiz, A. F. Izmaylov, J. L. Sonnenberg, D. Williams-Young, F. Ding, F. Lipparini, F. Egidi, J. Goings, B. Peng, A. Petrone, T. Henderson, D. Ranasinghe, V. G. Zakrzewski, J. Gao, N. Rega, G. Zheng, W. Liang, M. Hada, M. Ehara, K. Toyota, R. Fukuda, J. Hasegawa, M. Ishida, T. Nakajima, Y. Honda, O. Kitao, H. Nakai, T. Vreven, K. Throssell, J. A. Montgomery, J. E. Peralta Jr., F. Ogliaro, M. J. Bearpark, J. J. Heyd, E. N. Brothers, K. N. Kudin, V. N. Staroverov, T. A. Keith, R. Kobayashi, J. Normand, K. Raghavachari, A. P. Rendell, J. C. Burant, S. S. Iyengar, J. Tomasi, M. Cossi, J. M. Millam, M. Klene, C. Adamo, R. Cammi, J. W. Ochterski, R. L. Martin, K. Morokuma, O. Farkas, J. B. Foresman, and D. J. Fox, Inc. Gaussian, Wallingford CT, 2019., Gaussian 16, Revision C.01.
- [52] R. M. Parrish, L. A. Burns, D. G. A. Smith, A. C. Simmonett, A. E. DePrince, E. G. Hohenstein, U. Bozkaya, A. Y. Sokolov, R. Di Remigio, R. M. Richard, et al., Psi4 1.1: An open-source electronic structure program emphasizing automation, advanced libraries, and interoperability, *J. Chem. Theory Comput.* 13(7) (2017) 3185-3197.
- [53] MRCC, a quantum chemical program suite written by M. Kállay, P. R. Nagy, Z. Rolik, D. Mester, G. Samu, J. Csontos, J. Csóka, B. P. Szabó, L. Gyevi-Nagy, I. Ladjánszki, L. Szegedy, B. Ladóczki, K. Petrov, M. Farkas, P. D. Mezei, and B. Hégyel, see <http://www.mrcc.hu>.
- [54] Z. Rolik, L. Szegedy, I. Ladjanszki, B. Ladoczki, M. Kallay, An efficient linear-scaling CCSD(T) method based on local natural orbitals, *J. Chem. Phys.* 139(9) (2013).
- [55] T. H. Dunning Jr., Gaussian basis sets for use in correlated molecular calculations. I. The atoms boron through neon and hydrogen, *J. Chem. Phys.* 90(2) (1989) 1007-1023.
- [56] A. K. Wilson, T. van Mourik, T. H. Dunning Jr., Gaussian basis sets for use in correlated molecular calculations. VI. Sextuple zeta correlation consistent basis sets for boron through neon, *J. Mol. Struct.: THEOCHEM* 388 (1996) 339-349.
- [57] K. A. Peterson, T. H. Dunning Jr., Accurate correlation consistent basis sets for molecular core-valence correlation effects: The second row atoms Al–Ar, and the first row atoms B–Ne revisited, *J. Chem. Phys.* 117(23) (2002) 10548-10560.
- [58] T. H. Dunning, K. A. Peterson, A. K. Wilson, Gaussian basis sets for use in correlated molecular calculations. X. The atoms aluminum through argon revisited, *J. Chem. Phys.* 114(21) (2001) 9244-9253.
- [59] U. Bozkaya, C. D. Sherrill, Analytic energy gradients for the coupled-cluster singles and doubles



- with perturbative triples method with the density-fitting approximation, *J Chem Phys* 147(4) (2017).
- [60] C. Puzzarini, Accurate molecular structures of small- and medium-sized molecules, *Int. J. Quantum Chem.* 116(21) (2016) 1513-1519.
- [61] J. Noga, R. J. Bartlett, The full CCSDT model for molecular electronic structure, *J. Chem. Phys.* 86(12) (1987) 7041-7050.
- [62] G.E. Scuseria, H.F. Schaefer III, A new implementation of the full CCSDT model for molecular electronic structure, *Chem. Phys. Lett.* 152(4-5) (1988) 382-386.
- [63] J.D. Watts, R.J. Bartlett, The coupled-cluster single, double, and triple excitation model for open-shell single reference functions, *J. Chem. Phys.* 93 (1990) 6104-6105.
- [64] M. Kállay, P. R. Surján, Higher excitations in coupled-cluster theory, *J. Chem. Phys.* 115(7) (2001) 2945-2954.
- [65] W. Kutzelnigg, in: P. Schwerdtfeger (Ed.), *Relativistic Electronic Structure Theory. Part I. Fundamentals*, Elsevier, Amsterdam (2002).
- [66] I. M. Mills, 3.2 Vibration-Rotation Structure in Asymmetric-and Symmetric-Top Molecules, *Mol. Spectrosc.: Mod. Res.* 1 (1972) 115.
- [67] C. Gutle, J. Demaison, H. D. Rudolph, Anharmonic force field and equilibrium structure of nitric acid, *J. Mol. Spectrosc.* 254(2) (2009) 99-107.
- [68] M. Mendolicchio, E. Penocchio, D. Licari, N. Tasinato, V. Barone, Development and Implementation of Advanced Fitting Methods for the Calculation of Accurate Molecular Structures, *J. Chem. Theory Comput.* 13(6) (2017) 3060-3075.
- [69] V. Barone, Anharmonic vibrational properties by a fully automated second-order perturbative approach, *J. Chem. Phys.* 122(1) (2005) 014108.
- [70] J. Bloino, V. Barone, A second-order perturbation theory route to vibrational averages and transition properties of molecules: General formulation and application to infrared and vibrational circular dichroism spectroscopies, *J. Chem. Phys.* 136(12) (2012) 124108.
- [71] E. A. Orabi, G. H. Peslherbe, Computational insight into hydrogen persulfide and a new additive model for chemical and biological simulations, *Phys. Chem. Chem. Phys.* 21(29) (2019) 15988-16004.
- [72] A. D. Becke, Density-functional thermochemistry. III. The role of exact exchange, *J. Chem. Phys.* 98 (1993) 5648-52.
- [73] S. Grimme, Semiempirical hybrid density functional with perturbative second-order correlation, *J. Chem. Phys.* 124 (2006) 034108.
- [74] S. Grimme, S. Ehrlich, L. Goerigk, Effect of the damping function in dispersion corrected density functional theory, *J. Comput. Chem.* 32(7) (2011) 1456-1465.
- [75] E. Penocchio, M. Piccardo, V. Barone, Semiexperimental Equilibrium Structures for Building Blocks of Organic and Biological Molecules: The B2PLYP Route, *J. Chem. Theory Comput.* 11(10) (2015) 4689-4707.
- [76] C. Puzzarini, M. Heckert, J. Gauss, The accuracy of rotational constants predicted by high-level quantum-chemical calculations. I. molecules containing first-row atoms, *J. Chem. Phys.* 128(19) (2008).
- [77] V. Barone, M. Biczysko, J. Bloino, P. Cimino, E. Penocchio, C. Puzzarini, CC/DFT route toward accurate structures and spectroscopic features for observed and elusive conformers of flexible molecules: pyruvic acid as a case study, *J. Chem. Theory Comput.* 11(9) (2015) 4342-4363.

## Supporting Information

### **The Challenging Equilibrium Structure of HSSH: Another Success of the Rotational Spectroscopy / Quantum Chemistry Synergism**

Hexu Ye<sup>1</sup>, Marco Mendolicchio<sup>2</sup>, Holger Kruse<sup>3</sup>, Cristina Puzzarini<sup>4</sup>,  
Malgorzata Biczysko<sup>1,\*</sup> and Vincenzo Barone<sup>2,\*</sup>

<sup>1</sup> *International Centre for Quantum and Molecular Structures, Department of Physics,  
College of Sciences, Shanghai University, 99 Shangda Road, Shanghai, 200444 China*

<sup>2</sup> *Scuola Normale Superiore, Piazza dei Cavalieri 7, I-56126 Pisa, Italy*

<sup>3</sup> *Institute of Biophysics of the Czech Academy of Sciences, Královopolská 135, 612  
65 Brno, Czech Republic*

<sup>4</sup> *Dipartimento di Chimica “Giacomo Ciamician”, Università di Bologna,  
Via F. Selmi 2, 40126 Bologna, Italy*

#### **Contents:**

1. Table S1. Calculations with the valence and all electron correlation at CCSD(T) level.
2. Table S2.  $B_0^{\text{exp}}$ ,  $\Delta B_{\text{vib}}$  and  $\Delta B_{\text{el}}$  for HSSH. All data are in MHz.
3. Table S3. MAE and |MAX| of semi-experimental equilibrium structure of HSSH compare with best-CC-2 structure.
4. Table S4. XYZ coordinates of structures from theoretical and semi-experimental schemes.

**Table S1.** Calculation with the valence and all electron correlation at CCSD(T) level.

CVTZ	All electrons correlated	Frozen core	$\Delta^a$
SS(Å)	2.0678	2.0716	0.0038
SH(Å)	1.3402	1.3419	0.0017
HSS (deg)	97.94	97.95	0.00
HSSH (deg)	90.49	90.48	0.01
wCVTZ	All electrons correlated	Frozen core	$\Delta^b$
SS(Å)	2.0643	2.0689	0.0046
SH(Å)	1.3384	1.3402	0.0018
HSS (deg)	97.99	97.99	0.01
HSSH (deg)	90.50	90.49	0.01

<sup>a</sup>  $\Delta = \text{CCSD(T)/CVTZ/all electrons correlated} - \text{CCSD(T)/CVTZ/frozen core}$ ;<sup>b</sup>  $\Delta = \text{CCSD(T)/wCVTZ/all electrons correlated} - \text{CCSD(T)/wCVTZ/frozen core}$ .**Table S2.**  $B_0^{\text{exp}}$ ,  $\Delta B_{\text{vib}}$  and  $\Delta B_{\text{el}}$  for HSSH. All data are in MHz.

		$B_0^{\text{exp}}$	$\Delta B_{\text{vib}}(\text{cc-pVTZ})$					$\Delta B_{\text{el}}$
			B2PLYP	B2PLYP-D3BJ	B3LYP	B3LYP-D3BJ	MP2	MP2/cc-pVTZ
HSSH	A	146858.1658(11)	-1091.686	-1092.350	-1119.338	-1122.338	-1028.188	21.890
	B	6970.42679(15)	-46.367	-46.280	-45.322	-45.148	-46.151	-0.105
	C	6967.68576(14)	-47.274	-47.191	-46.082	-45.934	-47.396	-0.104
HS <sup>34</sup> SH	A	146694.9773(20)	-1029.589	-1046.522	-1053.295	-1089.823	-983.574	21.853
	B	6779.01770(15)	-45.207	-45.019	-44.762	-44.289	-44.759	-0.099
	C	6776.33850(27)	-46.059	-45.851	-45.570	-45.028	-45.807	-0.098
HSSD	A	100567.3952(14)	-562.283	-563.386	-570.070	-572.153	-537.837	10.131
	B	6826.36107(16)	-39.744	-39.662	-39.423	-39.262	-39.025	-0.100
	C	6677.79089(16)	-43.706	-43.629	-43.369	-43.215	-43.075	-0.096
DSSD	A	76459.8310(10)	-684.908	-682.783	-729.935	-724.123	-591.000	5.788
	B	6542.74398(14)	-37.082	-37.014	-36.826	-36.685	-36.634	-0.091
	C	6542.72004(14)	-29.286	-29.262	-29.015	-28.979	-28.843	-0.093
			$\Delta B_{\text{vib}}(\text{aug-cc-pVTZ})$					$\Delta B_{\text{el}}$
HSSH	A	146858.1658(11)	-1088.799	-1089.496	-1113.043	-1114.456	-1031.820	21.890
	B	6970.42679(15)	-46.420	-46.332	-45.283	-45.032	-46.268	-0.105
	C	6967.68576(14)	-47.234	-47.148	-45.876	-45.685	-47.553	-0.104
HS <sup>34</sup> SH	A	146694.9773(20)	-1052.964	-1052.248	-1090.960	-1087.325	-984.823	21.853
	B	6779.01770(15)	-45.122	-45.063	-44.322	-44.245	-44.863	-0.099
	C	6776.33850(27)	-46.037	-45.974	-45.126	-45.063	-45.962	-0.098
HSSD	A	100567.3952(14)	-559.975	-561.033	-566.413	-568.439	-538.646	10.131
	B	6826.36107(16)	-39.745	-39.662	-39.248	-39.078	-39.175	-0.100
	C	6677.79089(16)	-43.738	-43.660	-43.226	-43.068	-43.264	-0.096
DSSD	A	76459.8310(10)	-686.032	-683.883	-728.151	-722.288	-596.908	5.788
	B	6542.74398(14)	-29.353	-36.976	-28.941	-36.436	-29.033	-0.091

	C	6542.72004(14)	-37.043	-29.330	-36.580	-28.906	-36.864	-0.093
--	---	----------------	---------	---------	---------	---------	---------	--------

**Table S3.** MAE and |MAX| of semi-experimental equilibrium structure of HSSH compare with “best estimate” structure.

VTZ										
	$r_e^{SE}$					$r_e$				
	B2PLYP	B2PLYP-D3BJ	B3LYP	B3LYP-D3BJ	MP2	B2PLYP	B2PLYP-D3BJ	B3LYP	B3LYP-D3BJ	MP2
MAE <sup>a</sup>	0.0010	0.0009	0.0009	0.0009	0.0011	0.0156	0.0155	0.0229	0.0225	0.0076
MAX  <sup>a</sup>	0.0010	0.0010	0.0012	0.0013	0.0013	0.0264	0.0261	0.0356	0.0350	0.0151
MAE <sup>b</sup>	0.08	0.08	0.12	0.14	0.03	0.05	0.08	0.09	0.09	0.19
MAX  <sup>b</sup>	0.10	0.11	0.16	0.19	0.04	0.08	0.11	0.16	0.10	0.38
AVTZ										
	$r_e^{SE}$					$r_e$				
	B2PLYP	B2PLYP-D3BJ	B3LYP	B3LYP-D3BJ	MP2	B2PLYP	B2PLYP-D3BJ	B3LYP	B3LYP-D3BJ	MP2
MAE <sup>a</sup>	0.0009	0.0009	0.0008	0.0009	0.0010	0.0163	0.0161	0.0231	0.0227	0.0086
MAX  <sup>a</sup>	0.0011	0.0010	0.0014	0.0013	0.0011	0.0276	0.0273	0.0364	0.0358	0.0164
MAE <sup>b</sup>	0.10	0.07	0.12	0.12	0.08	0.09	0.09	0.19	0.11	0.36
MAX  <sup>b</sup>	0.11	0.08	0.16	0.12	0.09	0.16	0.14	0.19	0.12	0.42

<sup>a</sup> Mean absolute error (MAE) and maximum absolute deviations (|MAX|) with respect to the structure from “best estimate” method for bond lengths. <sup>b</sup> Mean absolute error (MAE) and maximum absolute deviations (|MAX|) with respect to the structure from “best estimate” method for angles.

**Table S4.** XYZ coordinates of structures from theoretical and semi-experimental schemes.

	best estimate		
	X	Y	Z
S	0.00000	0.00000	0.00000
S	0.00000	0.00000	2.05030
H	1.32587	0.00000	2.24089
H	-0.01481	-1.32579	-0.19059
	SE-B2PLYPD3BJ-AVTZ		
	X	Y	Z
S	0.00000	0.00000	0.00000
S	0.00000	0.00000	2.05130
H	1.32683	0.00000	2.24084
H	-0.01667	-1.32672	-0.18954

Results with other methods .xyz files, can be found in zipped attachment.

## Mol Files

[Click here to download Mol Files: h2s2\\_xyz files.rar](#)

**Declaration of interests**

☒ The authors declare that they have no known competing financial interests or personal relationships that could have appeared to influence the work reported in this paper.

☐The authors declare the following financial interests/personal relationships which may be considered as potential competing interests: